Telomere erosion in memory T cells induced by telomerase inhibition at the site of antigenic challenge in vivo

Reed, JR; Vukmanovic-Stejic, M; Fletcher, JM; Soares, MVD; Cook, JE; Orteu, CH; Jackson, SE; Birch, KE; Foster, GR; Salmon, M; Beverley, PCL; Rustin, MHA; Akbar, AN

The Journal of Experimental Medicine

Telomere Erosion in Memory T Cells Induced by Telomerase Inhibition at the Site of Antigenic Challenge In Vivo

John R. Reed,[1,2] Milica Vukmanovic-Stejic,[1] Jean M. Fletcher,[1] Maria Vieira D. Soares,[1] Joanne E. Cook,[1,3] Catherine H. Orteu,[2] Sarah E. Jackson,[1] Katie E. Birch,[1,2] Graham R. Foster,[4] Mike Salmon,[5] Peter C.L. Beverley,[3] Malcolm H.A. Rustin,[2] and Arne N. Akbar[1]

[1]*Department of Immunology and Molecular Pathology, Division of Infection and Immunity, University College London, London, W1T 4JF, England, UK*

[2]*Department of Dermatology, Royal Free Hospital, London, NW3 2QG, England, UK*

[3]*The Edward Jenner Institute for Vaccine Research, Compton, Berkshire, RG20 7NN, England, UK*

[4]*Hepatobiliary Group, Institute of Cell and Molecular Science, Queen Mary's School of Medicine and Dentistry, The Royal London Hospital, London, E1 1BB, England, UK*

[5]*Department of Rheumatology, Medical Research Council Centre for Immunoregulation, University of Birmingham, Birmingham, B15 2TT, England, UK*

Abstract

The extent of human memory T cell proliferation, differentiation, and telomere erosion that occurs after a single episode of immune challenge in vivo is unclear. To investigate this, we injected tuberculin purified protein derivative (PPD) into the skin of immune individuals and isolated responsive T cells from the site of antigenic challenge at different times. PPD-specific $CD4^+$ T cells proliferated and differentiated extensively in the skin during this secondary response. Furthermore, significant telomere erosion occurred in specific T cells that respond in the skin, but not in those that are found in the blood from the same individuals. Tissue fluid obtained from the site of PPD challenge in the skin inhibited the induction of the enzyme telomerase in T cells in vitro. Antibody inhibition studies indicated that type I interferon (IFN), which was identified at high levels in the tissue fluid and by immunohistology, was responsible in part for the telomerase inhibition. Furthermore, the addition of IFN-α to PPD-stimulated $CD4^+$ T cells directly inhibited telomerase activity in vitro. Therefore, these results suggest that the rate of telomere erosion in proliferating, antigen-specific $CD4^+$ T cells may be accelerated by type I IFN during a secondary response in vivo.

Key words: senescence • inflammation • differentiation • proliferation • cytokines

Introduction

The greater human longevity compared with that in mice indicates that human T cell memory will have to be maintained for much longer in vivo (1). This suggests that the persistence of human memory T cell pools may be subjected to additional constraints relative to animal systems. The majority of expanded T cells that are generated during an immune response are cleared by apoptosis to enable cellular homeostasis to be achieved during immune resolution. However, mechanisms that prevent the death of some cells have to be engaged to enable memory T cells to persist (2). The type I IFNs and cytokines that signal through the IL-2R common γ-chain are two groups of mediators that can induce activated T cell survival (2–4). Paradoxically, the antiapoptotic effects of these cytokines are also associated with chronic T cell–mediated inflammation in diseases such as rheumatoid arthritis and atopic eczema (5–7). Because this does not occur during normal immune resolution, additional control mechanisms that prevent excessive persistence of T cells at the end of an immune response must also exist.

J.R. Reed and M. Vukmanovic-Stejic contributed equally to this work.

Address correspondence to Arne N. Akbar, Dept. of Immunology and Molecular Pathology, Div. of Infection and Immunity, University College London, 46 Cleveland St., London W1T 4JF, England, UK. Phone: 44-207-679-9214; Fax: 44-207-679-9119; email: a.akbar@ucl.ac.uk

Abbreviations used in this paper: BCG, Bacille Calmette-Guerin; flow-FISH, flow cytometric detection of fluorescence in situ hybridization; HDA, heteroduplex analysis; MT, Mantoux test; PPD, purified protein derivative; SB, suction blister.

 J. Exp. Med. © The Rockefeller University Press • 0022-1007/2004/05/1433/11 $8.00
Volume 199, Number 10, May 17, 2004 1433–1443
http://www.jem.org/cgi/doi/10.1084/jem.20040178

It has been shown that the loss of replicative capacity due to telomere erosion can also regulate memory T cell maintenance (8). Telomeres are repeating hexameric sequences of DNA that are located at the ends of chromosomes (9). Each cell division leads to the loss of 50–100 bp of telomeric DNA due to the inability of DNA polymerase to fully replicate the ends of the chromosomes (10, 11). Although the induction of the enzyme telomerase during a primary response to antigen can compensate for telomere loss in antigen-specific T cells in vivo (12–14), upon repeated stimulation, T cells lose the ability to induce this enzyme, resulting in telomere erosion (15). This leads eventually to cell cycle arrest and replicative senescence; this is a mechanism that determines the residual replicative capacity of proliferating T cells (16–18).

The lack of suitable models has restricted investigations into mechanisms that regulate human memory T cells in vivo. This work was designed to establish an experimental system for the investigation of the kinetics of human memory T cell proliferation, differentiation, and telomere erosion during a secondary response to characterize factors that may regulate the persistence of these cells in situ. To do this, we injected purified protein derivative (PPD) into the skin of individuals who were immunized with Bacille Calmette-Guerin (BCG) to induce a secondary $CD4^+$ T cell response, also known as the Mantoux test (MT). Responding T cells were isolated from skin suction blisters (SBs) that were induced over these lesions at different times (19). We found that there was considerable proliferation of PPD-specific $CD4^+$ T cells during the secondary response in the skin and demonstrate that these cells differentiated to a $CD45RB^{lo}$ phenotype. Furthermore, we demonstrate for the first time that telomere erosion occurs in specific memory $CD4^+$ T cells during a secondary response in a nonlymphoid site and that this results in part from inhibition of telomerase in these cells by type I IFN in situ.

Materials and Methods

Volunteers. This work was approved by the Ethics Committee of the Royal Free Hospital. MT reactions were induced in healthy BCG-vaccinated volunteers on the flexor aspect of forearms by the intradermal injection of 0.1 ml of either 10 or 100 U/ml tuberculin PPD (Evans Vaccines Ltd.). Induration, palpability, and the change in erythema from baseline were measured and scored on day 3 and at the time of sampling as described previously (20). The MTs were sampled by skin biopsy or skin SB at an allotted time point between 0 and 19 d after PPD injection. One SB was induced in each of 100 individuals, who responded to the MT. In addition, for investigations into changes in T cell clonal distribution and telomere length, pairs of blisters were induced on 15 additional subjects that were harvested at two different time points. The mean age of the volunteers was 36.5 yr (10.4 ± SD). There was no significant difference in the median ages of individuals studied at each time point (Kruskal-Wallis test, $P > 0.99$). In addition, there was no difference in the number of males and females studied at each time point (χ^2 test, $P > 0.6$).

Skin SBs. Skin SBs were induced by the application of a negative pressure of 25–40 kPa (200–300 mmHg) below atmospheric pressure via a suction chamber for 2–4 h using a clinical suction pump (VP25; Eschmann) until a unilocular blister measuring 10–15 mm in diameter was formed. SBs were raised over the sites of PPD injection (MTs) or normal skin 18–24 h before sampling to ensure maximum cell recovery. The blister fluid was microcentrifuged at 650 *g* for 4 min to pellet the cells present. The pellet was resuspended in complete medium (RPMI 1640; Invitrogen and Life Technologies) containing 10% human AB serum, 100 U/ml penicillin, 100 μg/ml streptomycin, and 2 mM L-glutamine (all obtained from Sigma-Aldrich). Blister $CD4^+$ T cells were purified by negative selection. Blister cells were first incubated with antibodies against CD8, CD14, CD16 (Beckman Coulter), CD19, and glycophorin A (Beckman Coulter), and these cells were added to plates coated with rabbit anti–mouse immunoglobulins (DakoCytomation).

PBMC Preparation. Heparinized blood was collected from the same individuals at the time of blister aspiration. PBMCs were prepared by density centrifugation on Ficoll-Paque (Amersham Biosciences). $CD4^+$ T cells were isolated by positive or negative selection using the VARIO MACS (Miltenyi Biotec). $CD45RO^+$ populations were isolated by positive selection.

Flow Cytometric Analysis. Four-parameter analysis of T cell phenotype was performed on a FACSCalibur™ (Becton Dickinson) as described previously (21). Cells were enumerated after staining with fluorochrome-conjugated CD3, CD4, CD8, and/or Ki67 using TruCOUNT™ tubes (all obtained from Becton Dickinson). Other reagents were used as follows: CD45RA-FITC, IFN-γ–APC, IFN-γ–FITC, IL-2–FITC, and Ki67-FITC (all obtained from Becton Dickinson); and CD4-PE, CD45RA-PE, and CD45RB-FITC (all obtained from DakoCytomation).

Intracellular Cytokine Staining. SBs or PBMCs were stimulated with 10 μg/ml PPD (Statens Serum Institut) or 1:1,000 dilution tetanus toxoid (Aventis Pasteur MSD Ltd.) and incubated for 15 h at 37°C in a humidified 5% CO_2 atmosphere. 5 μg/ml brefeldin A (Sigma-Aldrich) was added after 2 h. Unstimulated controls were also included. The cells were fixed and permeabilized (Fix & Perm® Cell Permeabilisation Kit; Caltag Laboratories) before staining for CD3, CD4, IL-2, and IFN-γ.

Measurement of Telomere Length by Flow Cytometric Detection of Fluorescence In Situ Hybridization (Flow-FISH). Telomere length of $CD4^+$ T cells was measured using a modified two-color flow-FISH protocol (21). The cells were stained with CD4-biotin (Immunotech) followed by streptavidin-Cy3 (Cedarlane Laboratories Ltd.), after which samples were fixed and permeabilized (Fix & Perm® Cell Permeabilisation Kit; Caltag Laboratories). After washing in hybridization buffer, cells were incubated with 0.75 μg/ml of the PNA telomeric $(C_3TA_2)_3$ probe conjugated to Cy5. Samples were heated for 10 min at 82°C, rapidly cooled on ice, and hybridized for 1 h at room temperature in the dark. Samples were washed and analyzed immediately by flow cytometry. Fluorescently labeled beads (DakoCytomation) were used to standardize the cytometer settings. No probe controls were included to allow for differences in background fluorescence between samples. In addition, two cryopreserved PBMC samples with known telomere fluorescence were used as standards to ensure consistency of the results.

To measure telomere length of Ag-specific $CD4^+$ cells, we developed a three-color flow-FISH technique. SBs or PBMCs were stimulated with PPD for 15 h as aforementioned. After surface staining with CD4-biotin and streptavidin-Cy3, samples were fixed, permeabilized, and stained with IFN-γ–FITC before hybridization with the telomeric probe.

Telomerase Activity. Telomerase activity was measured using the telomeric repeat amplification protocol (TRAPeze Telomerase Detection Kit; Intergen Company). In brief, telomerase present in a test cell extract extends a template with telomeric repeats and, after PCR amplification, generates a ladder of products with 6-bp increments starting at 50 nucleotides. Samples were collected by the snap freezing of cells either recovered from SBs or from in vitro cultures at various time points after PPD injection or stimulation, respectively. Absolute numbers of $CD3^+Ki67^+$ cells in each sample were enumerated using Trucount tubes and Ki67 analysis. PCR was performed with samples adjusted to 500 $Ki67^+$ T cells per reaction. The negative control contains the PCR mix without cell extract, and the positive control contains an extract of a telomerase positive tumor cell line.

Type I IFN Inhibition Experiments. To investigate the effect of blister fluid on telomerase up-regulation in vitro, fresh day 3 blister fluid was added to 0.5 μg/ml PPD-stimulated PBMCs from the same donor (50% final dilution). In addition, autologous serum was also added to PPD-stimulated PBMCs as a control (25% final dilution). To block the effects of type I IFN, anti-CD118 antibody (anti–IFN-α, receptor chain 2; Calbiochem) or isotype control antibody (mouse IgG2a; Sigma-Aldrich) was added at 2.5 μg/ml to samples cultured in the presence of MT blister fluid. Samples for telomerase measurement were collected on day 3 after PPD stimulation, and proliferation was measured on day 5. To investigate the direct inhibition of telomerase activity by type I IFN in vitro, PPD-specific CD4 T cell lines generated from normal donors were restimulated in the presence of various doses of recombinant IFN-α (subtype 2a; R&D systems) or Roferon, a clinically used preparation of IFN-α (subtype 2a; Roche Pharmaceuticals). After 4 d, the cells were assayed for telomerase activity. Samples were adjusted to 500 $Ki67^+$ T cells per reaction as aforementioned.

Long-Term Cell Culture. Cells were isolated from blisters induced 19 d after PPD challenge in vivo and restimulated with PPD-pulsed, irradiated autologous PBMCs in vitro. Cell lines were maintained in complete medium supplemented with 5 ng/ml IL-2 and restimulated with 1 μg/ml PPD-pulsed autologous irradiated PBMCs every 10–14 d. Fresh medium and IL-2 were added every 3–4 d. Cell numbers and viability were quantified with Tru-count tubes. Population doublings (PD) were calculated using the following equation: PD = log (number of cells counted after expansion) − log (number of cells seeded)/log2.

Histological Analysis of Skin Biopsies. Frozen 6-μm sections of skin biopsies were fixed and immunostained using indirect immunoperoxidase, double indirect immunofluorescence, indirect alkaline phosphatase, and TUNEL methods as described previously (20). The number of positive cells was quantified by image analysis using a circular 100-μm diameter circular frame centered on the five largest perivascular infiltrates per section as described previously (20). Unconjugated anti–IFN-α antibody (C10F5; murine IgG1) was purchased from Serotec Ltd.

Measurement of Type I IFN in Blister Fluids. The amount of type I IFN in blister fluid was assayed by a standard antiviral assay (22). The concentration of type I IFN was determined by comparison with a standard curve prepared from IFN-α at known concentrations (IFN-α–N1, Wellferon; GlaxoSmithKline).

Assessment of Clonality by Heteroduplex Analysis (HDA). The clonal composition of purified $CD4^+$ T cells isolated from blisters at days 7 or 19 after PPD challenge in vivo or $CD4^+$ T cells from blood from the same volunteers was determined by comparing the CDR3 region of different TCR Vβ families. Blood $CD4^+$ T cells were collected at day 0 and cultured either with or without PPD and autologous irradiated PBMCs for 7 d in vitro. PCR was performed on 26 Vβ families (Vβ 1–24 including Vβ 5.1 and 5.2 and Vβ 13.1 and 13.2) using specific Vβ and common Cβ primers at each time point as described previously (23). Each sample PCR was mixed with Vβ-matched carrier DNA, denatured, and reannealed. The product was run on a 12% polyacrylamide gel, which was blotted and hybridized with a probe to the external Cβ region of the carrier. The probe was detected using anti–digoxigenin-AP Fab fragments and CDP-Star substrate (Roche Diagnostics). Identical clones within PBMCs and $CD4^+$ T cell populations were detected as heteroduplex bands with identical migration patterns (23). The presence of heteroduplices has been shown previously to relate to the presence of an expanded clone as determined by the sequencing of PCR product (23).

Results

A Human In Vivo Model of a Memory Immune Response. Healthy individuals who had been vaccinated previously against tuberculosis with BCG were selected for this analysis. The MT was induced by the intradermal injection of tuberculin PPD (Fig. 1 a). The clinical manifestation of this response was measured in terms of the change in erythema, size of induration, and palpability of the lesion, which peaked at 3 d after PPD injection, confirming previous papers (Fig. 1 b and references 5, 20). A novel observation was that the number of infiltrating T cells did not reach maximal levels until 7 d after PPD injection (Fig. 1 b). Therefore, the clinical and cellular peaks of this secondary response are asynchronous.

We adapted the skin SB technique to isolate leukocytes from the site of the MT at different times after PPD injection. Significantly higher numbers of leukocytes were obtained from the site of PPD injection (mean, 339,000; range, 5,000–1.5×10^6) at all time points compared with normal skin (mean, 50,830; range, 2,100–217,500; $P < 0.0001$). The maximum yield of cells in the SBs was found between days 2–3 compared with subsequent time points of the skin test reaction ($P < 0.0001$). However, no significant differences in yield were observed between days 5 and 19. Identical results were obtained when the yield was adjusted to the number of leukocytes per microliter of blister fluid to control for variations in blister size (unpublished data).

Lymphocytes constituted the majority of the leukocytes in SBs (Fig. 1 c), and >98% of these were $CD3^+$ T cells (not depicted). Other leukocytes found in the blister populations included $CD68^+$ monocytes and macrophages as well as smaller numbers of $CD1a^+$ Langerhans cells and DCs (unpublished data). The proportion of $CD4^+$ T cells increased significantly from 57.7 to 88% on days 3 and 19, respectively, after antigenic challenge (Kruskal-Wallis test; $P = 0.0006$), whereas expression in the peripheral blood did not change significantly during this period (Fig. 1 d). Greater than 95% of the $CD4^+$ T cells that were harvested from skin blisters or identified within biopsies were of the $CD45RA^-$ ($CD45RO^+$) primed/memory phenotype as compared with 50% of $CD4^+$ T cells in the blood (see Fig. 4 a), supporting previous observations that the MT is a $CD4^+$ memory, T cell–mediated immune response (5, 20).

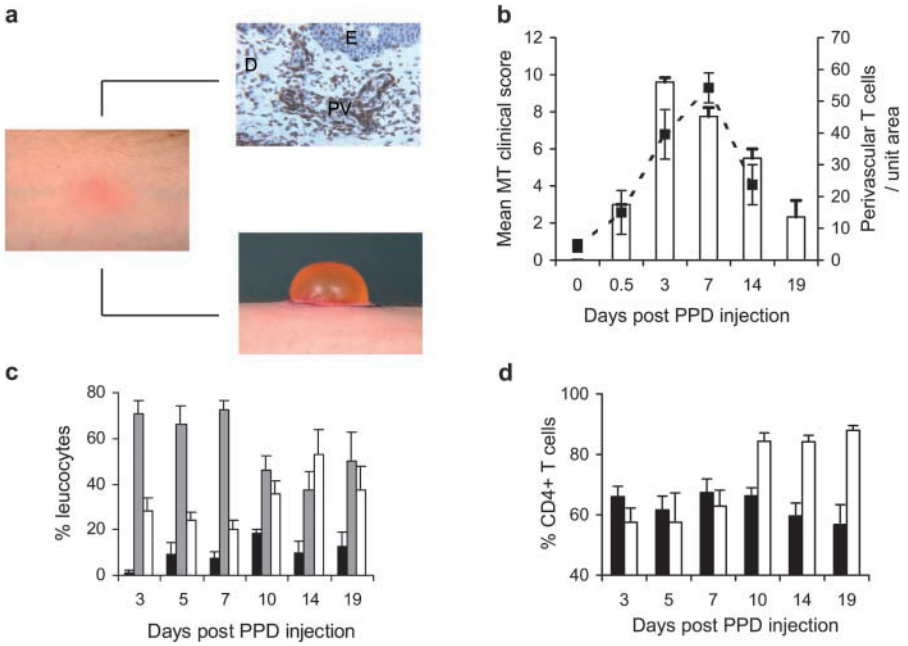

Figure 1. The Mantoux test (MT): a human in vivo model of a memory immune response. Samples were collected between 0 and 19 d after PPD injection (a, left). Skin biopsies were collected for immunohistochemistry, and the top right panel shows a day-3 MT skin section with a perivascular (PV) collection of $CD3^+$ T cells (E and D denote the epidermis and dermis, respectively; magnification, 20). Cutaneous lymphocytes were isolated from skin SBs that were induced over the sites of PPD injection at different times (a, bottom right). In panel b, the clinical score resulting from PPD challenge was measured at the time of sampling (□, left y axis), whereas the number of T cells within dermal perivascular infiltrates was determined by indirect immunoperoxidase staining (■, right y axis). The mean ± SEM of five experiments per time point is shown. In panel c, the percentage of granulocytes (black bars), lymphocytes (gray bars), and other leukocytes (white bars) isolated from SBs raised at different time points after PPD injection is shown. Leukocyte proportions were determined by flow cytometry. The mean ± SEM for three to six experiments per time point is shown. The percentage of $CD3^+$ T cells expressing CD4 in the peripheral blood (black bars) and blisters (white bars) during the course of the MT response was determined by flow cytometry (d). The mean ± SEM for four to seven experiments per time point is shown.

Specific $CD4^+$T Cells Proliferate at the Site of Antigenic Challenge. We evaluated the proportion of antigen-specific $CD4^+$ T cells that were isolated from the skin during the MT by their ability to synthesize IFN-γ after restimulation with PPD in vitro (Fig. 2 a). Minimal IFN-γ was synthesized when PPD was not added to the blister cells or when the cells were stimulated with tetanus toxoid (Fig. 2, a and b). Therefore, the cells that expressed IFN-γ were Ag-specific (PPD). We found a significant increase in these cells after intradermal challenge with PPD (Fig. 2 b; Kruskal-Wallis test; $P < 0.0001$). There was no increase in Ag-specific $CD4^+$ T cells in the blood, and these remained relatively constant at 0.5% of the $CD4^+$ T cell pool throughout the course of the response (Fig. 2 b). The maximum proportion of Ag-specific $CD4^+$ T cells detected after antigen challenge (32% of total $CD4^+$ T cells) was considerably higher than that predicted from previous studies (0.5–2%; reference 24). The proportion of $CD8^+$ Ag-specific T cells in the blisters did not increase during the course of the response and was <1% at all time points.

Next, we investigated whether proliferation of T cells in situ contributed to the accumulation of Ag-specific $CD4^+$ T cells after PPD injection. Tissue biopsies obtained from the site of antigen injection at different times were immunostained with the antibody to Ki67, which identifies cells in all phases of the cell cycle (Fig. 2 c; reference 25). We found that at day 7, at the time of maximal $CD4^+$ T cell accumulation, >20% of $CD4^+$ T cells were in cycle (Fig. 2, c and d). Similar proportions of proliferating $CD4^+$ T cells were identified by both immunohistochemistry in skin sections and by flow cytometry of blister cells taken at different time points. However, $Ki67^+$ $CD4^+$ T cells were not observed in blood at the same time points (unpublished data), indicating that the increase of PPD-specific $CD4^+$ T cells in the skin is mediated in part by proliferation of these cells in situ. We also found that there was an accumulation of apoptotic T cells during the course of the MT (Fig. 2 d). This indicates the dynamic nature of the response with both proliferation and death of $CD4^+$ T cells taking place at the site of antigenic challenge in vivo.

We are confident that the SB protocol actually samples cells that are responding in situ and not just those that are migrating away for the following reasons. First, the phenotype of $CD4^+$ T cells in tissue sections and SBs was identical ($CD45RO^+CD45RA^-$). Second, the proportions of $CD4^+$ T cells that were proliferating and the kinetics of proliferation were virtually identical when these cells were investigated by histology or in the blister samples, indicating that we were investigating the same responding population (Fig. 2 d). Third, the yield of cells obtained from blisters over the course of the aforementioned Mantoux reaction parallels the numbers of leukocytes that were observed by histology at different times after PPD injection (20).

Our results highlight that there is significant T cell activity long after the perceived clinical course of the skin test reaction. This is because previous studies have not generally sampled the skin beyond 4 d after antigen injection (19, 26). The continued T cell reactivity in the skin of our system between days 7 and 19 probably reflects both the continued presence of residual antigen and the expansion of these cells by cytokines that are present in situ (5, 20).

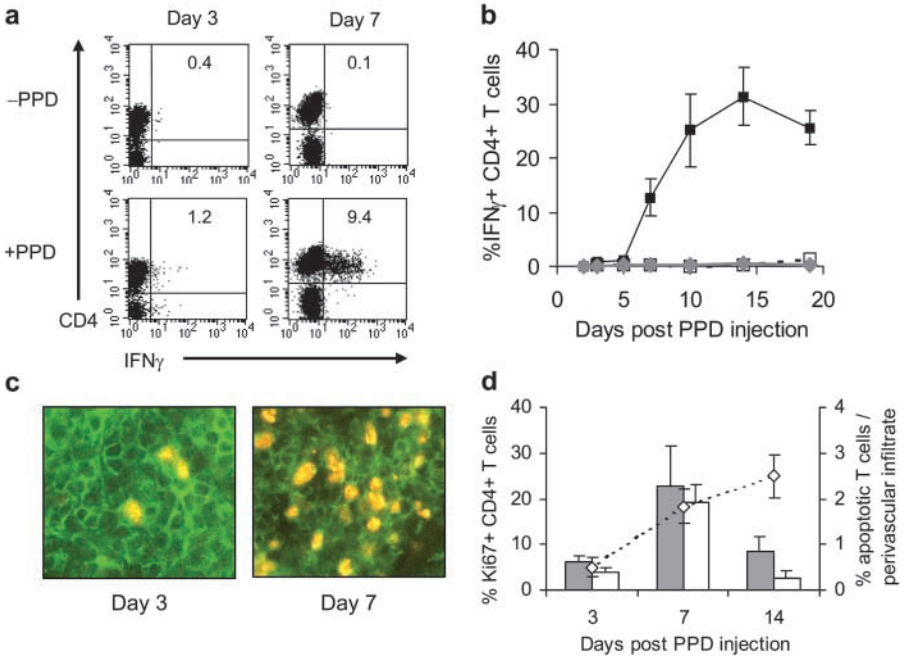

Figure 2. Antigen-specific CD4$^+$ T cell infiltration and proliferation in the skin during the MT. PBMCs and blister cells were stimulated with PPD, control antigen (tetanus toxoid), or left unstimulated for 15 h in the presence of brefeldin A. Representative dot plots of intracellular IFN-γ expression in days 3 and 7 blister cells are shown (a). The number in the top right quadrant of each dot plot indicates the percentage of CD4$^+$ T cells producing IFN-γ. (b) The proportion of IFN-γ–secreting (PPD-specific) CD4$^+$ T cells after PPD injection. The graph illustrates intracellular IFN-γ expression in PBMCs stimulated with PPD (gray diamonds) and blister cells stimulated with PPD (black squares) or tetanus toxoid (white squares). The mean ± SEM of 3–11 experiments performed at each time point is shown. Proliferating CD4$^+$ T cells in skin sections after PPD injection (c). Double immunofluorescence staining shows CD4$^+$ cells (green) and proliferating Ki67$^+$ cells (red; magnification, 20), whereas double positive Ki67$^+$CD4$^+$ cells are shown in yellow. (d) The percentage of proliferating Ki67$^+$ CD4$^+$ T cells in the skin after PPD challenge was determined by flow cytometry using blister cells (gray bars) and by double immunofluorescence in skin sections (white bars). The proportion of apoptotic (TUNEL$^+$) T cells in the perivascular infiltrates of skin sections was determined by double immunofluorescence (diamonds and dashed line). The mean ± SEM of three to five experiments performed at each time point is shown.

The Same CD4$^+$ T Cell Clones Persist during the Course of the MT. It was unclear how the turnover of CD4$^+$ T cells at the site of PPD injection affected the clonal composition of CD4$^+$ T cells during the course of the response. To assess potential changes in the clonal distribution, we used HDA (27). Unstimulated CD4$^+$ T cells from blood showed a polyclonal smear after HDA (Fig. 3 a). However, upon stimulation of these cells in vitro with PPD, clonal bands were detected (Fig. 3 a). CD4$^+$ T cells isolated from blisters on day 7 after PPD challenge showed a highly oligoclonal distribution (Fig. 3 a). Virtually all the clones identified in the blister samples at day 7 were also found in PPD-stimulated PBMCs from the same individuals (93–96%), indicating that the clonal bands in blister samples represented PPD-specific clones (Fig. 3 a). Of the clones identified in stimulated blood cells, only 66% (range 44–85%) were present in the skin at day 7, suggesting that not all CD4$^+$ T clones that were found in blood could enter or survive in the skin.

Next, we investigated the clonal relationship between CD4$^+$ T cells that were isolated from pairs of skin blisters in the same individuals that were induced over the sites of PPD injection at days 7 and 19. We measured the total number of clones that were found in 26 different Vβ families. We identified 44 ± 14 clonal bands on day 7 (mean ± SEM of four individuals) and 40 ± 15 at day 19 (Fig. 3 b). Clonality during the course of the PPD response remained relatively stable with 80% of the clones (range 57–94%) that were identified at day 19 also being present at day 7 (Fig. 3 b). The 20% of clones that were found on day 19, but that were not observed on day 7, probably represented recently expanded populations. Although 74% of clones that were found at day 7 were also present at day 19, there were 26 ± 15% (range 9–43%) of clones that were not present, suggesting that some clones are lost during the MT. Overall, this points to a dynamic picture in which the vast majority of PPD-specific clones in the skin are maintained during

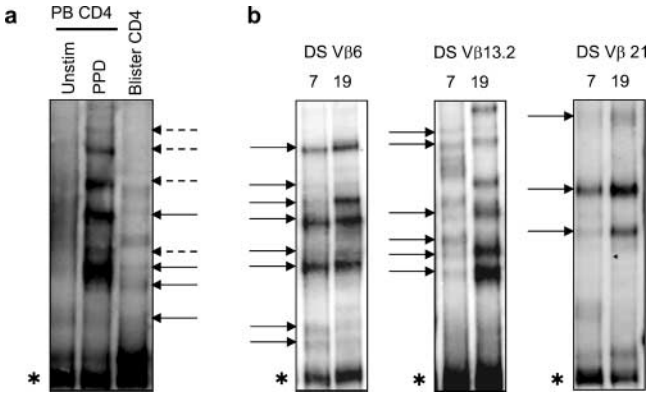

Figure 3. Clonal analysis of CD4$^+$ T cells in the skin during the MT. HDA of purified blood and blister CD4$^+$ T cells was performed for the 26 Vβ families (a). Unstimulated blood CD4$^+$ T cells (Unstim), blood CD4$^+$ T cells stimulated with PPD in vitro for 7 d (PPD), and blister CD4$^+$ T cells from a day 7 MT (Blister CD4) collected from the same individual were compared. One representative Vβ family from one out of five volunteers that were investigated is shown. Solid-line arrows indicate clonal bands shared between PPD-stimulated blood CD4$^+$ T cells and blister cells. Dashed-line arrows indicate clonal bands that are only present in the PPD-stimulated blood CD4$^+$ T cells. HDA was performed for 26 different Vβ families on purified blister CD4$^+$ T cells isolated from paired MTs on days 7 and 19 (b). Arrows on the left of each gel indicate clonal bands that are present in the blisters at both time points. Three representative Vβ families from one out of four volunteers are shown. The asterisks on each gel indicate the position of the carrier homoduplex.

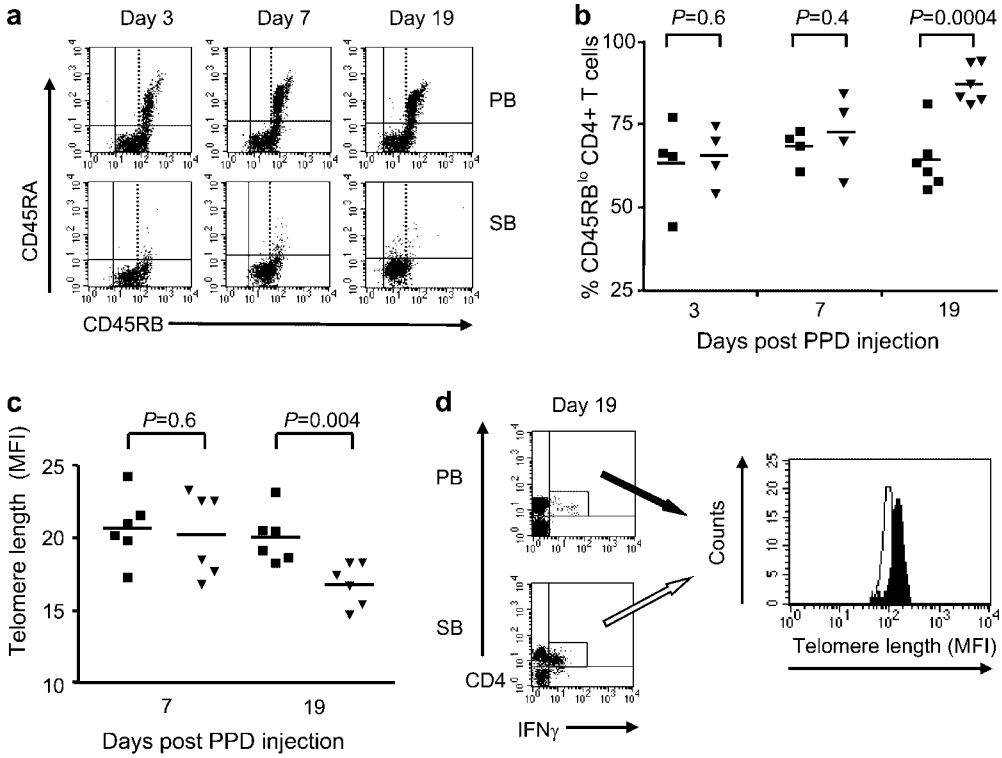

Figure 4. Differentiation of $CD4^+$ T cells in the skin during the MT. Representative dot plots of CD45RA and CD45RB expression on blood (PB) and suction blister (SB) $CD4^+$ T cells on different days after PPD challenge (a). The dotted line defines the gate between CD45RB high and low expression. (b) The percentage of highly differentiated $CD4^+$ memory T cells (defined as $CD45RA^-$, $CD45RB^{lo}$) in the blood (■) and skin blisters (▼) during the MT. The horizontal line denotes the mean. p-values were calculated using the paired Student's *t* test. The telomere length of blood (■) and skin (▼) $CD4^+CD45RO^+$ T cells was determined during the MT (c). The telomere length of $CD4^+$ T cells from blood and SBs at days 7 and 19 after PPD injection was determined by two-color flow-FISH. The horizontal line denotes the mean. p-values were calculated using the paired Student's *t* test. The telomere length of PPD-specific blood and skin $CD4^+$ T cells 19 d after MT induction was determined by three-color flow-FISH (d). The histogram shows the telomere length (mean fluorescence intensity [MFI]) of PPD-specific (as defined by IFN-γ production) $CD4^+$ T cells in the blood (shaded histogram) and blister (unshaded histogram). The data represent one out of two experiments with identical results that were performed.

the course of the immune response. However, some clonal evolution also occurs that may be due to the proliferation, apoptosis, and also migration of some specific $CD4^+$ T cells in and out of the immune response in situ (Fig. 2 d).

$CD4^+$ T Cells Differentiate in the Skin during a Secondary Response. We investigated CD45RB expression as an indication of the extent of $CD4^+$ T cell differentiation in situ. This molecule is highly expressed in $CD45RA^+CD4^+$ naive T cells, but shows bimodal distribution on primed/memory $CD45RA^-RO^+$ $CD4^+$ T cells (28). Memory $CD4^+$ T cells that are $CD45RB^{low}$ are more differentiated and have shorter telomeres compared with those that are $CD45RB^{high}$ cells (unpublished data).

During the course of the MT, virtually all the $CD4^+$ T cells isolated from the skin were $CD45RA^-CD45RO^+$ in contrast with the $CD4^+$ population from blood from the same individuals, where many $CD45RA^+$ T cells were observed (Fig. 4 a). When we compared CD45RB expression on $CD45RA^-CD45RO^+$ (primed) $CD4^+$ T cells from blood and blisters in the same individuals on days 3 and 7 during the induction and peak phases of the response, respectively, no difference was observed (Fig. 4 b). However, by day 19, a significantly greater number of $CD4^+$ T cells from the skin showed low CD45RB expression compared with equivalent populations from paired blood samples. This indicated that primed Ag-specific $CD4^+$ T cells undergo further differentiation in situ after PPD challenge (Fig. 4 b). To confirm this, we measured the telomere length of $CD4^+$ T cells in the skin using flow-FISH (21). Because all $CD4^+$ T cells in the skin blisters are $CD45RO^+$, we compared their telomere lengths with blood $CD4^+CD45RO^+$ T cells. At day 7 after PPD injection, the telomere length of $CD4^+$ T cells in the SBs was similar to that found in $CD4^+CD45RO^+$ T cells from blood samples in the same individuals (Fig. 4 c). However, by day 19, the telomere length of $CD4^+$ T cells from the skin was significantly shorter than the equivalent population in blood, confirming that they were more differentiated. The decrease in telomere mean fluorescence intensity in blister samples observed at day 19 equates to the loss of 0.4 kb of telomeric DNA as determined using calibration curves correlating telomere length (in kilobases) measured by Southern blot analysis with the flow-FISH technique as described previously (21).

We developed a three-color flow-FISH technique, which involves gating on IFN-γ^+CD4^+ T cells after short-term ex vivo stimulation with PPD, followed by flow-FISH staining for telomeres (Fig. 4 d). This technique demonstrated that PPD-specific $CD4^+$ T cells at the site of antigenic stimulation had shorter telomeres compared with PPD-specific $CD4^+$ T cells from blood in the same individuals. Therefore, Ag-specific T cell proliferation and differentiation occurs at the site of secondary immune challenge in the skin in humans (Fig. 4 d).

Telomerase Activity in the Skin. We investigated whether telomere erosion in $CD4^+$ T cells after PPD stimulation in

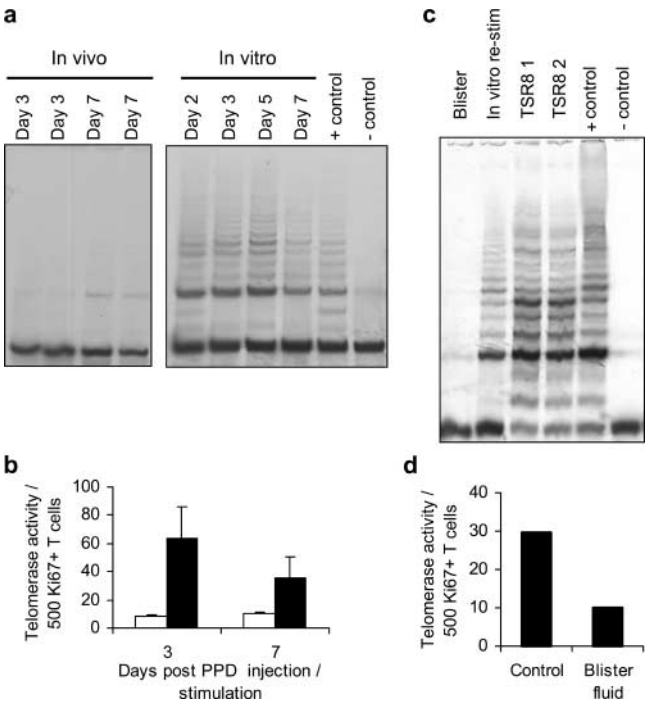

Figure 5. Low telomerase activity in CD4$^+$ T cells in the skin after PPD stimulation in vivo. Telomerase activity in T cells isolated from SBs after PPD injection in two different individuals on days 3 and 7 after PPD injection (in vivo) and also from blood CD4$^+$ T cells from one individual at different times after PPD stimulation in vitro (a). Telomerase activity (total product generated) per 500 Ki67$^+$ proliferating T cells isolated from MTs (b, white bars) and PBMCs stimulated in vitro with PPD (black bars). The mean ± SEM of three experiments is shown. Skin CD4$^+$ T cells can up-regulate telomerase activity when stimulated with PPD in vitro (c). T cells were isolated from day 3 MTs, and telomerase activity was determined in T cells immediately upon isolation (Blister), whereas the remaining cells were stimulated with PPD in vitro for 3 d (In vitro re-stim). Data are representative of four experiments performed. The negative control contains the PCR mix without cell extract, and the positive control contains an extract of a telomerase-positive tumor cell line. TSR8 denotes the internal quantitative control. Day 3 blister fluid suppresses telomerase activity (d). PBMCs were stimulated with PPD in vitro in the presence of autologous serum as a control or autologous blister fluid that was obtained from day 3 MT. Telomerase activity per 500 Ki67$^+$ T cells was measured on day 3. The data are representative of three experiments performed.

vivo resulted from lack of telomerase induction in these cells. At days 3 and 7 after PPD challenge, there was extensive CD4$^+$ T cell cycling as 7.7 ± 2.0% and 17.8 ± 6.2% of these cells, respectively, were Ki67$^+$. The extent of cell cycling was greater than that observed when CD4$^+$ T cells from blood were stimulated by PPD in vitro for 3 and 7 d, respectively (2.4 ± 0.4% and 9.7 ± 4.0% Ki67$^+$). Because telomerase is only up-regulated in the activated proliferating population of T cells (29, 30), we standardized telomerase assays to include an equivalent number of Ki67$^+$ T cells in each sample. For the first time, this allowed a direct comparison of the activity of this enzyme in cycling CD4$^+$ T cells from both blood and blister at different times after stimulation (30, 31). Telomerase activity was minimal in cycling CD4$^+$ T cells that were isolated from the skin compared with CD4$^+$ T cells from blood that were stimulated by PPD in vitro (Fig. 5, a and b). This indicated that telomere erosion in PPD-specific CD4$^+$ T cells was linked to the lack of telomerase activity in these cells in vivo.

To determine if the lack of telomerase in Ag-specific CD4$^+$ T cells was due either to inherent inability to induce this enzyme or to active inhibition of this enzyme in situ, we isolated blister cells 3 d after PPD challenge and investigated their ability to up-regulate telomerase activity after PPD stimulation in vitro (Fig. 5 c). As before, there was very little telomerase activity in freshly isolated cycling blister T cells; however, there was a fivefold increase in telomerase when these cells were restimulated in vitro (Fig. 5 c). This suggested that telomerase was actively inhibited in situ, but that this inhibition was reversible. This was confirmed by inhibiting telomerase activity of PPD-stimulated blood derived CD4$^+$ T cells in vitro, with blister fluid obtained at day 3 from the site of PPD injection from the same donor (Fig. 5 d).

Type I IFN within the MT Inhibits Telomerase Induction. Our previous studies indicate that type I IFN (IFN-α and IFN-β) can regulate the rate of differentiation of human T cells (32). Together with reports that IFN-α can inhibit the activity of telomerase in tumor cell lines in vitro (33), this prompted us to determine whether this group of cytokines was responsible for the inhibition of telomerase activity in PPD-specific CD4$^+$ T cells in the skin in situ. By immunohistological analysis, we identified cells that expressed high levels of IFN-α in the perivascular infiltrates of skin sections 3 d after PPD challenge (Fig. 6 a). High uniform levels of expression were also detected in keratinocytes (Fig. 6 a). This was confirmed by measurement of peak concentrations of type I IFN in SB fluid that was obtained at day 3 after PPD injection (Fig. 6 b). This coincided with the time at which telomerase was greatest in CD4$^+$ T cells that were PPD-stimulated in vitro, but absent from cycling CD4$^+$ T cells in the skin (Fig. 5 b).

The telomerase activity of PPD-stimulated CD4$^+$ T cells obtained from peripheral blood was much lower when these cells were cultured with blister fluid from a day-3 MT relative to culture with autologous serum (Fig. 6 c). We added an antibody directed to the second subunit of the type I IFN receptor (anti–IFN-R2), which blocks the signaling by all forms of type I IFN, to PPD stimulated T cells that were cultured with day 3 blister fluid. An isotype control antibody was also added to identical cultures. The IFN-R2 antibody induced a fivefold enhancement of telomerase activity in these cultures, whereas the addition of a control antibody had little effect (Fig. 6 c). Furthermore, we showed that the addition of clinically used preparations of IFN-α (Roferon) or recombinant IFN-α at concentrations similar to that found in blister fluid directly blocked the induction of telomerase activity in PPD-stimulated T cells in a dose-dependent manner in vitro (Fig. 6 d). In addition, IFN-β could also block telomerase activity in PPD-stimulated T cells (unpublished data). We do not rule out the possibility that other members of the type I IFN family, such as limitin (22, 34), or other factors may also contribute in part to telomerase inhibition in the skin during a Mantoux reaction.

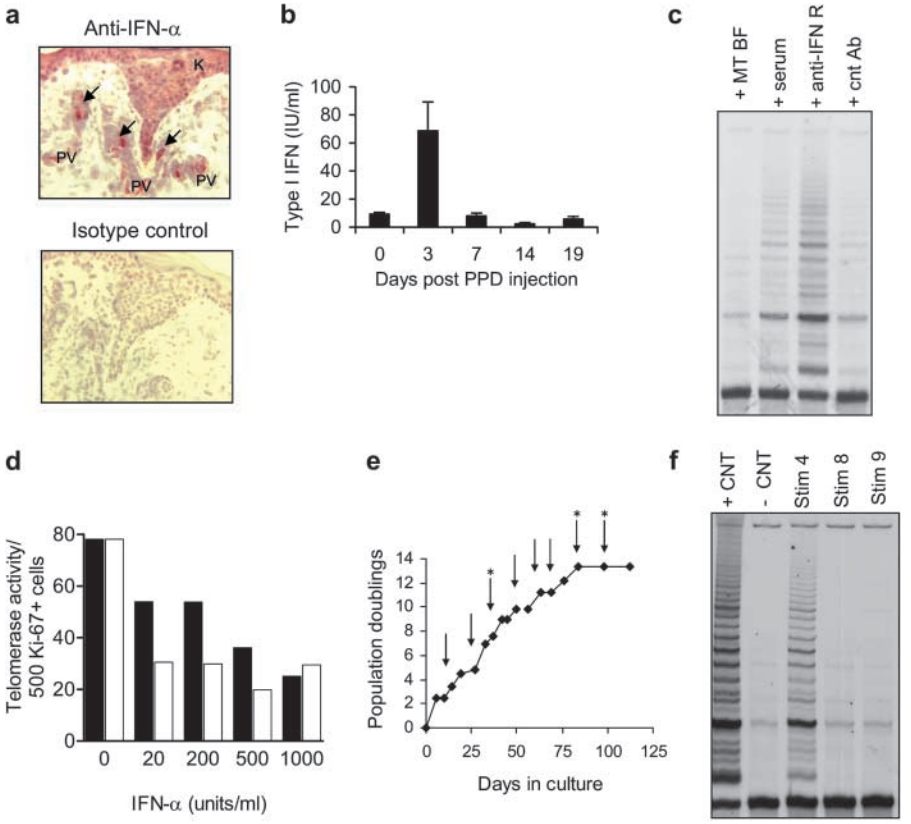

Figure 6. Type I IFN in blister fluid inhibits telomerase activity in PPD-stimulated T cells. IFN-α–producing cells present in day 3 MT skin sections were identified using indirect alkaline phosphatase staining (a, top). The bottom panel shows staining with an isotype control (magnification, 20). Keratinocytes (K) and isolated cells within the perivascular infiltrates (PV; indicated by arrows) expressed IFN-α. (b) The presence of type I IFN in blister fluid collected at different times after MT induction. The data represent the mean ± SEM of type I IFN in blister samples from five different individuals assayed per time point. Type I IFN mediates the suppression of telomerase activity induced by day 3 blister fluid (c). PBMCs were stimulated with PPD in vitro in the presence of autologous day 3 blister fluid (+MT BF) or autologous serum (+serum). Blocking antibody reactive with type I IFN receptor 2 (CD118; +anti-IFN R) or isotype control antibody (+cnt Ab) were added to cultures stimulated in the presence of MT blister fluid. Samples were collected 3 d after stimulation, and samples were adjusted to 500 proliferating Ki67$^+$ T cells per reaction for telomerase analysis (one out of three representative experiments is shown). Direct inhibition of telomerase activity by type I IFN (d). A PPD-specific CD4$^+$ T cell line was restimulated with PPD in the presence of recombinant IFN-α (black bars) or Roferon (white bars), a clinical preparation of IFN-α for 4 d. Samples were adjusted so that telomerase activity was measured in an equivalent number of cycling (Ki67$^+$) T cells (one of three representative experiments is shown). Blister-derived CD4$^+$ T cells can expand in vitro (e). Cells recovered from a day-19 blister were stimulated in vitro with PPD-pulsed irradiated autologous PBMCs as APCs. Arrows indicate each point of restimulation in vitro. The asterisks indicate points when samples were collected to measure telomerase activity. Telomerase activity of CD4$^+$ T cells isolated from day 19 blisters decreases with repeated stimulation in vitro (f). Samples were collected on day 4 after each point of PPD restimulation. Telomerase activity per 500 Ki67$^+$ T cells was determined as before. Stim 4, Stim 8, and Stim 9 indicate the 4th, 8th, and 9th stimulations with PPD and irradiated APCs in vitro.

Next, we examined the capacity of CD4$^+$ T cells that were removed from the skin microenvironment to expand in response to repeated stimulation with PPD stimulation in vitro (Fig. 6 e). These cells were able to expand in culture, and this was associated with their ability to up-regulate telomerase after restimulation in vitro (Fig. 6 f). However, despite the optimal stimulation of the skin-derived CD4$^+$ T cells with PPD in vitro, the cells reached replicative senescence at day 125 after eight episodes of restimulation, after which no further expansion of the cells occurred (Fig. 6 d). This was associated with the loss of telomerase inducibility in these cells (Fig. 6 e). The loss of telomerase activity in the repeatedly stimulated cells was not reversed by the addition of anti–IFN-R2 antibodies (unpublished data), suggesting that a different mechanism of telomerase down-regulation was in operation.

Discussion

Most studies on human memory T cell differentiation and proliferation have been performed on peripheral blood–derived populations, but the actual sites where these events occur in vivo are poorly defined. To clarify this, we characterized an experimental system for investigating the initiation and resolution phases of a human CD4$^+$ T cell–mediated secondary response to antigen in vivo. Using this model, we demonstrate that there is an increase in PPD-specific CD4$^+$ T cells during the course of this response in the skin that is largely due to the expansion of T cell clones that were present early in the response in situ. This is in contrast with previous studies in mice where Ag-specific T cell proliferation only occurred in lymphoid, but not in nonlymphoid, tissues (35–37). These conflicting results may be due to the fact that we investigated a secondary response, whereas the studies in mice related to primary responses (35, 36).

The intense proliferative activity was accompanied by an increase in CD4$^+$ T cell apoptosis during the course of the response, indicating that there was extensive T cell turnover during this secondary response in the skin. Previous studies using histological investigation of Mantoux lesions indicate that the proliferation during this turnover may be driven in part by the presence of IL-2 and IL-15 within the skin after PPD injection (5). However, the apoptosis that was observed was induced by different mechanisms at the peak and resolution phases of the response (5). Although the death of the proliferating CD4$^+$ T cells at the height of the response was linked to activation-induced cell death as-

sociated with elevated expression of CD95L, the apoptosis during the resolution phase was linked to cytokine starvation associated with down-regulation of the antiapoptotic molecule Bcl-2 (5). Because >80% of the $CD4^+$ T cell clones that were found 21 d after PPD injection were also present early in the response at day 7, it is likely that proliferation and death are both occurring within the same antigen-specific T cell population that is responding to PPD within the skin.

We have made several unexpected observations in this work. First, the kinetics of the clinical response to PPD injection is different from the kinetics of antigen-specific T cell infiltration. Although the former peaks at 2–3 d when very few antigen-specific $CD4^+$ T cells are present, the latter peaks between 7–15 d, when the clinical response is markedly reduced. The events that lead to the recruitment of the specific cells require further investigation. A second new observation was that antigen-specific $CD4^+$ T cells were differentiating within the skin after PPD injection. This was indicated by the significant proliferation and loss of CD45RB expression by the responding $CD4^+$ T cell population. The down-regulation of CD45RB by human $CD4^+$ T cells has been previously shown to be associated with profound changes in the capacity for cytokine secretion (28). The functional changes that accompany the differentiation of PPD-specific $CD4^+$ T cells in the skin are currently under investigation.

Telomeres have been shown to erode as cells undergo extensive proliferation and T cells from elderly individuals have shorter telomeres than young subjects (15). However, the extent to which telomeres in memory T cells erode after a single secondary challenge with antigen is unknown. Therefore, it is of considerable interest that we observed an average loss of 400 bp of telomere DNA in the $CD4^+$ T cells that were responding in the skin 3 wk after the injection of PPD. Because telomeres in human $CD4^+$ T cells have been shown to decrease by an average of 50 bp/yr, this loss of telomeres was equivalent to that expected after 8 yr of normal aging in vivo (8, 18). At this rate of telomere erosion, one prediction would be that cells that continuously proliferate in the skin would reach senescence rapidly, where growth arrest occurs because telomeres are unable to fulfil their protective function (9). However, the investigation of antigen-specific T cells in draining and nondraining lymph nodes of telomerase-deficient mice (38) and animals with short telomeres (of equivalent length to that in humans; reference 12) will be required to assess directly whether telomere erosion limits uncontrolled T cell proliferation during secondary responses in vivo.

The accelerated telomere erosion during the secondary response in the skin was due in part to the active, but reversible, inhibition of telomerase in proliferating T cells by type I IFN. Immunohistological analysis showed that a constituent of the type I IFN that was detected at day 3 after PPD challenge was IFN-α. However, IFN-β has also been shown previously to be present at day 3 during this response (5). Because all the type I IFNs signal through the same receptor (39), we do not exclude the possibility that more than one member of this family of mediators contributes to telomerase inhibition. Although telomerase activity in $CD4^+$ T cells that were stimulated with PPD in vitro was substantially inhibited by the addition of type I IFN, we could not completely inhibit the activity of this enzyme with these cytokines. Extremely low telomerase activity that was found in proliferating cells in the skin suggests that other factors may also contribute to inhibition of this enzyme in the antigen-specific cells in vivo.

Although telomerase activity in T cells is inhibited by type I IFN, it can be up-regulated in some T cells by cytokines such as IL-7 (40). These results clearly demonstrate that different cytokines may have a profound impact on the replicative lifespan of T cells. Apart from cytokine-mediated regulation of telomerase, intrinsic down-regulation of enzymatic activity occurs in T cells that are activated repeatedly and may be related to end-stage differentiation (9, 10). Telomerase inhibition by this second pathway is irreversible, but senescence in these cells can be bypassed by telomerase transfection (41, 42). The signaling pathways that lead to telomerase down-regulation after repeated stimulation or after addition of type I IFN are poorly defined but may involve inhibition of CD28 expression (16), transcriptional regulation, capacity for enzyme translocation from cytoplasm to the nucleus, and also chromatin remodelling of the telomerase gene (15). These pathways require further investigation as they may provide targets for manipulating the retention or loss of specific T cells in vivo.

In summary, we demonstrate that antigen-specific $CD4^+$ T cells can differentiate extensively outside lymphoid tissue during a secondary response in humans in vivo. This indicates that it is essential to investigate immune responses within the context of the tissue where they are taking place. Although this poses significant constraints on the study of human immunity, the use of appropriate animal models, such as telomerase (38) or type I IFNR-deficient animals (4), will enable the clarification of specific questions that relate to human T cell differentiation during secondary responses in vivo.

We thank Profs. A. Mitchison and C. Buckley and Dr. D. Mosser for discussions. We are grateful to all the volunteers who took part in this work.

This work was funded by grants from the Biotechnology and Biological Sciences Research Council Experimental Research on Aging Initiative, Research Into Aging, The Sir Jules Thorne Research Trust, and The Hayward Foundation and Dermatrust.

Submitted: 28 January 2004
Accepted: 12 April 2004

References

1. Akbar, A.N., M.V. Soares, F.J. Plunkett, and M. Salmon. 2000. Differential regulation of CD8+ T cell senescence in mice and men. *Mech. Ageing Dev.* 121:69–76.
2. Akbar, A.N., and M. Salmon. 1997. Cellular environments and apoptosis: tissue microenvironments control activated T-cell death. *Immunol. Today.* 18:72–76.

3. Pilling, D., A.N. Akbar, J. Girdlestone, C.H. Orteu, N.J. Borthwick, N. Amft, D. Scheel-Toellner, C.D. Buckley, and M. Salmon. 1999. Interferon-beta mediates stromal cell rescue of T cells from apoptosis. *Eur. J. Immunol.* 29:1041–1050.
4. Marrack, P., J. Kappler, and T. Mitchell. 1999. Type I interferons keep activated T cells alive. *J. Exp. Med.* 189:521–530.
5. Orteu, C.H., M.H. Rustin, E. O'Toole, C. Sabin, M. Salmon, L.W. Poulter, and A.N. Akbar. 2000. The inhibition of cutaneous T cell apoptosis may prevent resolution of inflammation in atopic eczema. *Clin. Exp. Immunol.* 122: 150–156.
6. McInnes, I.B., J. al Mughales, M. Field, B.P. Leung, F.P. Huang, R. Dixon, R.D. Sturrock, P.C. Wilkinson, and F.Y. Liew. 1996. The role of interleukin-15 in T-cell migration and activation in rheumatoid arthritis. *Nat. Med.* 2:175–182.
7. Salmon, M., D. Scheel-Toellner, A.P. Huissoon, D. Pilling, N. Shamsadeen, H. Hyde, A.D. D'Angeac, P.A. Bacon, P. Emery, and A.N. Akbar. 1997. Inhibition of T cell apoptosis in the rheumatoid synovium. *J. Clin. Invest.* 99:439–446.
8. Rufer, N., T.H. Brummendorf, S. Kolvraa, C. Bischoff, K. Christensen, L. Wadsworth, M. Schulzer, and P.M. Lansdorp. 1999. Telomere fluorescence measurements in granulocytes and T lymphocyte subsets point to a high turnover of hematopoietic stem cells and memory T cells in early childhood. *J. Exp. Med.* 190:157–167.
9. Blackburn, E.H. 2001. Switching and signaling at the telomere. *Cell.* 106:661–673.
10. Harley, C.B., A.B. Futcher, and C.W. Greider. 1990. Telomeres shorten during ageing of human fibroblasts. *Nature.* 345:458–460.
11. Kipling, D., and H.J. Cooke. 1990. Hypervariable ultra-long telomeres in mice. *Nature.* 347:400–402.
12. Maini, M.K., M.V. Soares, C.F. Zilch, A.N. Akbar, and P.C. Beverley. 1999. Virus-induced CD8+ T cell clonal expansion is associated with telomerase up-regulation and telomere length preservation: a mechanism for rescue from replicative senescence. *J. Immunol.* 162:4521–4526.
13. Soares, M.V., F.J. Plunkett, C.S. Verbeke, J.E. Cook, J.M. Faint, L.L. Belaramani, J.M. Fletcher, N. Hammerschmitt, M. Rustin, W. Bergler, et al. 2004. Integration of apoptosis and telomere erosion in virus-specific CD8+ T cells from blood and tonsils during primary infection. *Blood.* 103:162–167.
14. Hathcock, K.S., S.M. Kaech, R. Ahmed, and R.J. Hodes. 2003. Induction of telomerase activity and maintenance of telomere length in virus-specific effector and memory CD8+ T cells. *J. Immunol.* 170:147–152.
15. Hodes, R.J., K.S. Hathcock, and N.P. Weng. 2002. Telomeres in T and B cells. *Nat. Rev. Immunol.* 2:699–706.
16. Valenzuela, H.F., and R.B. Effros. 2002. Divergent telomerase and CD28 expression patterns in human CD4 and CD8 T cells following repeated encounters with the same antigenic stimulus. *Clin. Immunol.* 105:117–125.
17. Effros, R.B., and G. Pawelec. 1997. Replicative senescence of T cells: does the Hayflick Limit lead to immune exhaustion? *Immunol. Today.* 18:450–454.
18. Weng, N.P., B.L. Levine, C.H. June, and R.J. Hodes. 1995. Human naive and memory T lymphocytes differ in telomeric length and replicative potential. *Proc. Natl. Acad. Sci. USA.* 92:11091–11094.
19. Pitzalis, C., G.H. Kingsley, M. Covelli, R. Meliconi, A. Markey, and G.S. Panayi. 1991. Selective migration of the human helper-inducer memory T cell subset: confirmation by in vivo cellular kinetic studies. *Eur. J. Immunol.* 21:369–376.
20. Orteu, C.H., L.W. Poulter, M.H. Rustin, C.A. Sabin, M. Salmon, and A.N. Akbar. 1998. The role of apoptosis in the resolution of T cell-mediated cutaneous inflammation. *J. Immunol.* 161:1619–1629.
21. Plunkett, F.J., M.V. Soares, N. Annels, A. Hislop, K. Ivory, M. Lowdell, M. Salmon, A. Rickinson, and A.N. Akbar. 2001. The flow cytometric analysis of telomere length in antigen-specific CD8+ T cells during acute Epstein-Barr virus infection. *Blood.* 97:700–707.
22. Foster, G.R., and N.B. Finter. 1998. Are all type I human interferons equivalent? *J. Viral Hepat.* 5:143–152.
23. Maini, M.K., L.R. Wedderburn, F.C. Hall, A. Wack, G. Casorati, and P.C. Beverley. 1998. A comparison of two techniques for the molecular tracking of specific T-cell responses; CD4+ human T-cell clones persist in a stable hierarchy but at a lower frequency than clones in the CD8+ population. *Immunology.* 94:529–535.
24. Kalish, R.S., and K.L. Johnson. 1990. Enrichment and function of urushiol (poison ivy)-specific T lymphocytes in lesions of allergic contact dermatitis to urushiol. *J. Immunol.* 145:3706–3713.
25. Gerdes, J., H. Lemke, H. Baisch, H.H. Wacker, U. Schwab, and H. Stein. 1984. Cell cycle analysis of a cell proliferation-associated human nuclear antigen defined by the monoclonal antibody Ki-67. *J. Immunol.* 133:1710–1715.
26. Platt, J.L., B.W. Grant, A.A. Eddy, and A.F. Michael. 1983. Immune cell populations in cutaneous delayed-type hypersensitivity. *J. Exp. Med.* 158:1227–1242.
27. Maini, M.K., N. Gudgeon, L.R. Wedderburn, A.B. Rickinson, and P.C. Beverley. 2000. Clonal expansions in acute EBV infection are detectable in the CD8 and not the CD4 subset and persist with a variable CD45 phenotype. *J. Immunol.* 165:5729–5737.
28. Salmon, M., D. Pilling, N.J. Borthwick, N. Viner, G. Janossy, P.A. Bacon, and A.N. Akbar. 1994. The progressive differentiation of primed T cells is associated with an increasing susceptibility to apoptosis. *Eur. J. Immunol.* 24:892–899.
29. Bodnar, A.G., N.W. Kim, R.B. Effros, and C.P. Chiu. 1996. Mechanism of telomerase induction during T cell activation. *Exp. Cell Res.* 228:58–64.
30. Hiyama, K., Y. Hirai, S. Kyoizumi, M. Akiyama, E. Hiyama, M.A. Piatyszek, J.W. Shay, S. Ishioka, and M. Yamakido. 1995. Activation of telomerase in human lymphocytes and hematopoietic progenitor cells. *J. Immunol.* 155:3711–3715.
31. Weng, N.P., B.L. Levine, C.H. June, and R.J. Hodes. 1996. Regulated expression of telomerase activity in human T lymphocyte development and activation. *J. Exp. Med.* 183:2471–2479.
32. Borthwick, N.J., M. Lowdell, M. Salmon, and A.N. Akbar. 2000. Loss of CD28 expression on CD8(+) T cells is induced by IL-2 receptor gamma chain signalling cytokines and type I IFN, and increases susceptibility to activation-induced apoptosis. *Int. Immunol.* 12:1005–1013.
33. Xu, D., S. Erickson, M. Szeps, A. Gruber, O. Sangfelt, S. Einhorn, P. Pisa, and D. Grander. 2000. Interferon alpha down-regulates telomerase reverse transcriptase and telomerase activity in human malignant and nonmalignant hematopoietic cells. *Blood.* 96:4313–4318.
34. Oritani, K., P.W. Kincade, C. Zhang, Y. Tomiyama, and Y. Matsuzawa. 2001. Type I interferons and limitin: a comparison of structures, receptors, and functions. *Cytokine Growth*

Factor Rev. 12:337–348.
35. Harris, N.L., V. Watt, F. Ronchese, and G. Le Gros. 2002. Differential T cell function and fate in lymph node and non-lymphoid tissues. *J. Exp. Med.* 195:317–326.
36. Reinhardt, R.L., D.C. Bullard, C.T. Weaver, and M.K. Jenkins. 2003. Preferential accumulation of antigen-specific effector CD4 T cells at an antigen injection site involves CD62E-dependent migration but not local proliferation. *J. Exp. Med.* 197:751–762.
37. Ely, K.H., L.S. Cauley, A.D. Roberts, J.W. Brennan, T. Cookenham, and D.L. Woodland. 2003. Nonspecific recruitment of memory CD8+ T cells to the lung airways during respiratory virus infections. *J. Immunol.* 170:1423–1429.
38. Rudolph, K.L., S. Chang, H.W. Lee, M. Blasco, G.J. Gottlieb, C. Greider, and R.A. DePinho. 1999. Longevity, stress response, and cancer in aging telomerase-deficient mice. *Cell.* 96:701–712.
39. Mogensen, K.E., M. Lewerenz, J. Reboul, G. Lutfalla, and G. Uze. 1999. The type I interferon receptor: structure, function, and evolution of a family business. *J. Interferon Cytokine Res.* 19:1069–1098.
40. Soares, M.V., N.J. Borthwick, M.K. Maini, G. Janossy, M. Salmon, and A.N. Akbar. 1998. IL-7-dependent extrathymic expansion of CD45RA+ T cells enables preservation of a naive repertoire. *J. Immunol.* 161:5909–5917.
41. Hooijberg, E., J.J. Ruizendaal, P.J. Snijders, E.W. Kueter, J.M. Walboomers, and H. Spits. 2000. Immortalization of human CD8+ T cell clones by ectopic expression of telomerase reverse transcriptase. *J. Immunol.* 165:4239–4245.
42. Rufer, N., M. Migliaccio, J. Antonchuk, R.K. Humphries, E. Roosnek, and P.M. Lansdorp. 2001. Transfer of the human telomerase reverse transcriptase (TERT) gene into T lymphocytes results in extension of replicative potential. *Blood.* 98:597–603.